

## Inelastic Incoherent Neutron Scattering Measurements of Intact Cells and Tissues and Detection of Interfacial Water

Robert C. Ford,<sup>\*,†</sup> Stuart V. Ruffle,<sup>‡</sup> Anibal J. Ramirez-Cuesta,<sup>§</sup> Ilias Michalarias,<sup>#</sup> Ilir Beta,<sup>#</sup> Aline Miller,<sup>||</sup> and Jichen Li<sup>#</sup>

Contribution from the Departments of Biomolecular Sciences, Physics, and Chemical Engineering, UMIST, Manchester M60 1QD, U.K., School of Biological and Chemical Sciences, University of Exeter, Exeter EX4 4QG, U.K., and ISIS, Rutherford Appleton Laboratory, Chilton, Didcot, Oxfordshire, OX11 0QX, U.K.

Received October 30, 2003; E-mail: r.ford@umist.ac.uk

**Abstract:** We have previously used inelastic incoherent neutron scattering spectroscopy to investigate the properties of aqueous suspensions of biomolecules as a function of hydration. These experiments led to the identification of signals corresponding to interfacial (hydration) water at low water content. A prediction from these studies was that in the crowded environment inside living cells, a significant proportion of the water would be interfacial, with profound implications for biological function. Here we describe the first inelastic incoherent neutron scattering spectroscopy studies of living cells and tissues. We find that the interfacial water signal is similar to that observed for water interacting with purified biomolecules and other solutes, i.e., it is strongly perturbed in the librational and translational intermolecular optical regions of the spectrum at 20–150 meV. The ratio of interfacial water compared to total water in cells (~30%) is in line with previous experimental data for hydration water and calculations based on simple assumptions.

### Introduction

Cells are environments with extremely high macromolecule concentrations.<sup>1–4</sup> Levels of protein around 300 mg/mL have been reported in vivo for eukaryotic cells. In contrast, in vitro studies of proteins rarely take place at concentrations above 1–10 mg/mL. The effects of molecular crowding in vivo have been explored from theoretical calculations and from in vitro experiments using molecular crowding agents,<sup>1–4</sup> but there have been fewer experimental studies of crowding in vivo. Measurement of diffusional motion of biomolecules in cells is possible using various techniques, and comparisons have been made between motion of a given macromolecule within a cell with its motion in a dilute aqueous environment.<sup>3</sup> Most measurements report that diffusion for macromolecules in vivo is around 25% of that in free solution, although lower values may be possible (a value of 9% has been obtained for green fluorescent protein (GFP) in *Escherichia coli* cells<sup>3</sup>).

Excluded volume effects, as described by Minton and others<sup>1–4</sup> predict many of the effects of molecular crowding in vivo, but other physical factors need to be considered. For example, a potential outcome of molecular crowding may be exerted via effects on the properties of cellular water molecules.

We have previously found that interfacial water molecules within a few hydration shells of biomembranes and DNA molecules show a drastically altered inelastic neutron scattering spectrum,<sup>5,6</sup> with energy shifts in the librational (60–120 meV) and O–H stretching bands (400–450 meV) as well as a disappearance of the two translational intermolecular optical peaks at 28 and 38 meV that have been associated with water–water hydrogen bonding in bulk water.<sup>7,8</sup> Similarly, quasi-elastic neutron scattering measurements of interfacial water showed a reduced diffusion dynamics versus bulk water.<sup>9–12</sup> Evidence that the organization and properties of water molecules at the interface with biological macromolecules are different than those of pure water has also been obtained from X-ray crystallography of biomolecules.<sup>13–15</sup> Water properties are relevant to many biological phenomena such as protein folding and stability, DNA

- (5) Ruffle, S. V.; Michalarias, I.; Li, J. C.; Ford, R. C. *J. Am. Chem. Soc.* **2002**, *124*, 565–569.
- (6) Beta, I. A.; Kolesnikov, A. I.; Michalarias, I.; Wu, G. L.; Ford, R. C.; Li, J. C. *Can. J. Phys.* **2003**, *81*, 367–371.
- (7) Li, J. C. *J. Chem. Phys.* **1996**, *105*, 6733–6755.
- (8) Li, J. C.; Tomkinson, J. In *Molecular Dynamics from Classical to Quantum Methods*; Balbuena, P. B., Seminario, J. M., Eds.; Theoretical and Computational Chemistry, Vol. 7; Elsevier: Amsterdam, 1999; pp 471–512.
- (9) Beta, I. A.; Michalarias, I.; Li, J. C.; Ford, R. C.; Bellissent-Funel, M.-C. *Chem. Phys.* **2003**, *292*, 451–454.
- (10) Dellerue, S.; Bellissent-Funel, M. C. *Chem. Phys.* **2000**, *258*, 315–325.
- (11) Russo, D.; Baglioni, P.; Peroni, E.; Teixeira, J. *Chem. Phys.* **2003**, *292*, 235–245.
- (12) Pieper, J.; Charalambopoulou, G.; Steriotis, T.; Vasenkov, S.; Desmedt, A.; Lechner, R. E. *Chem. Phys.* **2003**, *292*, 465–476.
- (13) Esposito, L.; Vitagliano, L.; Sica, F.; Sorrentino, G.; Zagari, A.; Mazzarella, L. *J. Mol. Biol.* **2000**, *297*, 713–792.
- (14) Clark, G. R.; Squire, C. J.; Baker, L. J.; Martin, R. F.; White, J. *Nucleic Acids Res.* **2000**, *28*, 1259–1265.
- (15) Soler-Lopez, M.; Malinia, L.; Subirana, J. A. *J. Biol. Chem.* **2000**, *275*, 23034–23044.

<sup>†</sup> Department of Biomolecular Sciences, UMIST.

<sup>‡</sup> University of Exeter.

<sup>§</sup> Rutherford Appleton Laboratory.

<sup>#</sup> Department of Physics, UMIST.

<sup>||</sup> Department of Chemical Engineering, UMIST.

(1) Ellis, J. R. *Curr. Opin. Struct. Biol.* **2001**, *11*, 114–119.

(2) Burg, M. C. *Cell. Physiol. Biochem.* **2000**, *10*, 251–256.

(3) Verkman, A. S. *Trends Biochem. Sci.* **2002**, *27*, 27–33.

(4) Hall, D.; Minton, A. P. *Biochim. Biophys. Acta* **2003**, *1649*, 127–139.

packaging, molecular recognition, and cellular tolerance of freezing. Since most cellular functions and chemistry occur in water solution, it seems likely that crowding could have a profound effect on the chemistry of life via its influence on water. If macromolecular crowding alters the properties of a significant fraction of the water in the cell, then it could exert a strong influence on the behavior of smaller solutes via a water effect as well as influencing macromolecules via the excluded volume effect.<sup>1–4</sup>

## Methods

Incoherent inelastic neutron scattering (IINS) measurements were carried out on the TOSCA instrument at the ISIS facility at the Rutherford Appleton Laboratory (U.K.). TOSCA is currently the world's highest resolution indirect geometry inelastic vibrational neutron scattering spectrometer.<sup>16–18</sup> Neutrons are scattered by all atomic nuclei, and in the case of incoherent inelastic scattering (which is the type of scattering here) the scattering is from single centers, and therefore, there can be no interference of scattered waves. Neutrons lose energy by exciting vibrational modes of the scatterer; hence, an IINS spectrum is an energy loss spectrum. The data were recorded over the range 2–500 meV (16–4000 cm<sup>-1</sup>) with a resolution of 1 to 1.5% of the energy transferred ( $\Delta E/E$ ) (below 100 cm<sup>-1</sup> the resolution was approximately constant,  $\sim 8$  cm<sup>-1</sup>) and reflected the vibrational spectrum of a substance. All molecular vibrations are neutron-active because the nuclear interactions are not subject to dipole or polarizability selection rules and all vibrations are therefore, in principle, observable. The scattering intensity is linearly proportional to the concentration of the scatterer and its cross section. Because the scattering cross section is much greater for hydrogen (80 barn) than for any other element (normally less than 5 barn), displacements involving hydrogen dominate in neutron spectroscopy. The liquid samples were measured in standard aluminum cans 50 × 40 × 1 mm<sup>3</sup>, and solid or paste samples were enclosed in aluminum foil sachets. The spectra were recorded below 20 K (to minimize multiphonon contributions which are significant at high temperature) using an automatic sample changer that can handle 24 samples at a time. Both back-scattered and forward-scattered neutrons were recorded, although only the backscattering data (which has better resolution than the forward bank of detectors) was used for the analysis. The data were unbinned except for the chymotrypsin samples. The background from the aluminum cans was subtracted as a matter of routine, although this was a very small contribution (<1% of the intensity) and was featureless.

Data equivalent to 1600  $\mu\text{A}\cdot\text{h}$  (ca. 9 h collection time on TOSCA) were acquired for all the cells and tissues samples, while a high signal/noise bulk water spectrum used for subtraction was recorded equivalent to 3900  $\mu\text{A}\cdot\text{h}$ . Subtraction of this ice Ih (bulk water) signal from the spectra of samples containing interfacial water was performed such that the large sharp edge at 67 meV (that is absent in the interfacial water spectrum) was minimized in the difference spectrum, which involved the scaling of the ice Ih spectrum accordingly. A minor residual spike remained in some difference spectra because of small errors in the time-of-flight measurement between different runs. Estimates of the interfacial water and total water components were obtained by integrating over the librational band (45–130 meV) in the difference spectrum and then comparing this to the integrated librational peak in the original spectrum. The original (unsubtracted) spectrum and the difference spectrum contained a small contribution in this region due to the nonwater components of the sample (see Figures 1 and 2).

The major contribution from biomolecules in the IINS spectra was around 170 meV, where a broad peak due to a mixture of –CH and –NH motions was observed.<sup>5,16–18</sup> Subtraction of the nonwater component (giving a double-difference spectrum) was carried out where beam time allowed the recording of a spectrum for the lyophilized sample (see Results section).

Cardiac muscle tissue was prepared by dissection of fresh beef heart (obtained from a local abattoir) to remove major blood vessels and connective tissue. A sample equivalent to  $\sim 3$ –5 g of muscle tissue was dissected as a slice  $\sim 3$  mm in width and 20 mm × 40 mm across. After being enclosed in an aluminum foil sachet, the sample was rapidly frozen by being plunged into liquid nitrogen. Beetroot (*Beta vulgaris*) was grown outdoors, and freshly harvested material was dissected to generate a uniform slab  $\sim 3$  mm thick and 20 mm × 40 mm wide extracted from the center of the beetroot tuber. After being enclosed in an aluminum foil sachet, the sample was frozen by being plunged into liquid nitrogen as above. Baker's yeast (*Saccharomyces cerevisiae* w.t.) was obtained commercially as a hydrated paste, and samples (4–5 g) were loaded into an aluminum foil sachet and frozen as above. A sample was separately prepared and dried by freeze-drying under vacuum. Spinach leaves were obtained from a local market. After the stems were removed and the leaves were de-ribbed to remove the major veins, several leaves were superimposed and enclosed in an aluminum foil sachet. *Chlamydomonas reinhardtii* cells (3 L) were grown in the laboratory in Tris-acetate-phosphate (TAP) medium to a cell density of  $5 \times 10^6$  mL<sup>-1</sup> as described in ref 19 and harvested by centrifugation at 3500g at room temperature, which yielded  $\sim 21$  g of wet cell paste. The pellets from the centrifugation step were resuspended in either TAP or TAP plus 3% v/v methanol. Repeat centrifugation at 3500g was carried out, and after decanting the supernatant, the pellets were transferred to aluminum foil sachets, each containing 4–5 g of wet cell paste and frozen as described below. Some remaining cells from each treatment were assayed for viability after freezing. These cells were resuspended at room temperature in either TAP or TAP plus 3% methanol, at  $5 \times 10^6$  cells/mL, frozen at a rate of 1 °C min<sup>-1</sup> for 70 min, and subsequently stored in liquid nitrogen. After 1 week, cells were thawed at 35 °C for 2 min in a water bath, transferred into TAP growth liquid media for 12 h, and then plated onto TAP-agar containing 50 mg/dm<sup>3</sup> ampicillin and grown at 22 °C with illumination of 110  $\mu\text{einsteins m}^{-2} \text{ s}^{-1}$ . Counting of colonies appearing on the plates after 10 days was carried out to determine the percent of surviving cells. Aqueous solutions consisting of sucrose, TAP, or methanol were loaded into flat aluminum cans sealed with indium wire.

Lyophilized, salt-free chymotrypsin (bovine type II) was purchased from Sigma plc. Any residual water was removed by vacuum desiccation until no further mass change occurred. The chymotrypsin data were recorded over  $\sim 6$  h (equivalent to 1000  $\mu\text{A}\cdot\text{hr}$ ), and because of the lower quantity of the samples (1 g of dry protein or 1 g of protein plus 0.7 g of water), the data were averaged into 1 meV bins. The latter averaging did not compromise the resolution of the instrument.

Environmental scanning electron microscopy (ESEM) images were collected using an FEI Quanta 400 instrument with a Peltier sample stage and gaseous secondary electron detector (GSED). All samples were contained within a circular brass stub with a diameter of 1 cm and a depth of 0.5 cm, and the temperature was controlled using the Peltier cooling stage with a water/propanol coolant maintained at 283 K. Prior to initiating pump down of the chamber from ambient to a few Torr, the sample was left for a few minutes to allow temperature equilibration. During the pump down procedure, images from the CCD camera confirmed that the sample remained stable, i.e., there was no “boiling” of water during this process as the method adopted (pumping down in steps) ensured that a high percentage of water vapor remained in the sample chamber/environment. In all cases, the sample was cooled

(16) Goupil-Lamy, A. V.; Smith, J. C.; Yunoki, J.; Parker, S. F.; Kataoka, M. *J. Am. Chem. Soc.* **1997**, *119*, 9268–9273.

(17) Middendorf, H. D.; Hayward, R. L.; Parker, S. F.; Bradshaw, J.; Miller, A. *Biophys. J.* **1995**, *69*, 660–673.

(18) Colognesi, D.; Celli, M.; Cillico, F.; Newport, R. J.; Parker, S. F.; Rossi-Albertini, V.; Sacchetti, F.; Tomkinson, J.; Zoppi, M. *Appl. Phys. A* **2002**, *74* (Suppl.), S64–66.

(19) Harris, E. H. In *The Chlamydomonas Source Book*; Academic Press: San Diego, CA, 1989.

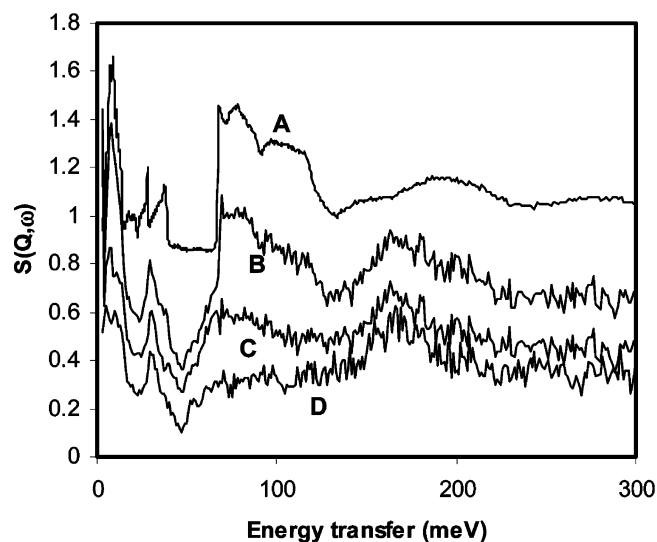


**Figure 1.** Inelastic incoherent neutron scattering spectra. Trace A shows the high signal/noise spectrum of bulk water (ice Ih) with no binning of the data. Trace B shows a pure protein (chymotrypsin) mixed with water at a ratio of 0.7 g water/g protein. The spectrum is a mixture of bulk water, interfacial water, and protein components. Trace C shows the result after subtraction of the bulk water component, leaving the interfacial water (broad peak 45–130 meV) signal as well as protein signals. Trace D shows the spectrum for “dry” chymotrypsin, revealing the protein contributions.

to  $\sim 275$  K ( $2^\circ\text{C}$ ) and surrounded by water vapor at a pressure of ca. 4 Torr. Working distances were typically 8–10 mm, and images were collected using an accelerating voltage of 10 keV. Under such conditions, signal-to-noise ratio was maximized, sample dehydration was minimized, and detailed high-resolution images were obtained.

## Results

Figure 1, trace A, shows a very high signal/noise IINS spectrum of bulk water (ice Ih form). The high-energy resolution of the instrument is indicated by the very sharp peaks and edges, especially by the translational intermolecular optical modes at 28.4 and 37.9 meV and the librational band lower-energy edge at 67.0 meV. The IINS spectrum of a protein (chymotrypsin) mixed with water at a ratio of (10:7 w/w) is shown as trace B in Figure 1. The spectrum shares some features of the water spectrum described above, but has additional broad peaks at  $\sim 170$  and  $\sim 30$  meV due to protein.<sup>16,17</sup> Moreover, the chymotrypsin sample displays the interfacial water signal in the librational region indicated by the broadening and lower-energy shift of the librational edge.<sup>5</sup> The strong difference between the interfacial water signal and the bulk water signal allows accurate subtraction of the bulk water signal, as displayed in trace C. This trace illustrates the very broad interfacial water signal in the librational region, which is closely comparable to those presented earlier for hydrated DNA, gelatin, and proteolipid membranes.<sup>5–6,20–22</sup> In addition, we found that the two sharp peaks in the molecular optic region are lost in the interfacial water signal, again in agreement with DNA and membrane samples. The protein’s contributions to the IINS spectra can be appreciated by examination of trace D, which represents freeze-dried chymotrypsin. There is perhaps still some residual water

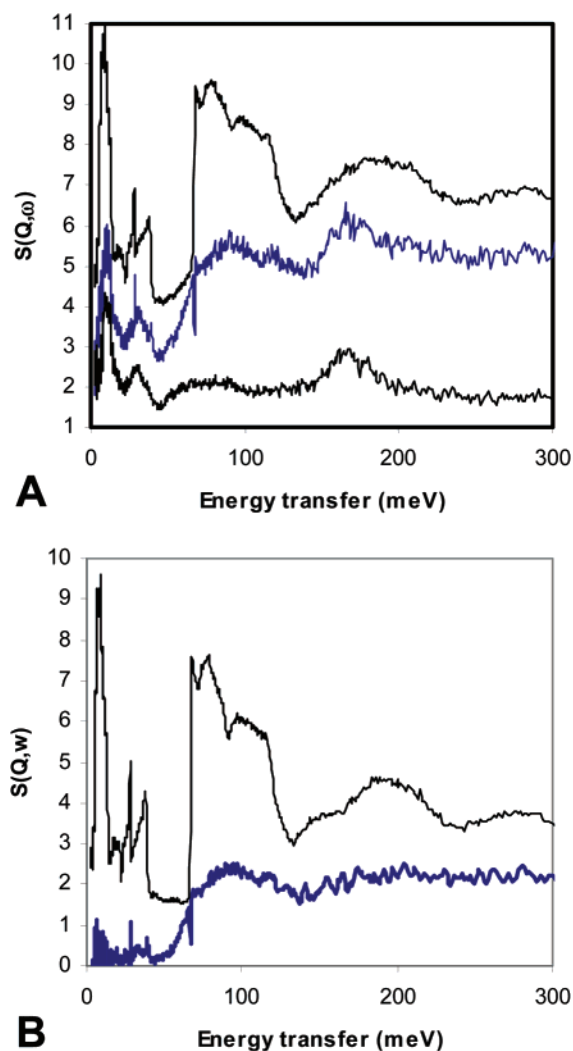


**Figure 2.** (A). Inelastic incoherent neutron scattering spectra of yeast cells. The upper trace shows a hydrated yeast cell paste which is dominated by components arising from bulk water (ice Ih spectrum; see Figure 1). The size of this spectrum is reduced by a factor of 2 compared to the other two spectra to facilitate comparison. A contribution from interfacial water can be observed by the broadening and shifting to lower energy of the librational peak around 50–60 meV. Subtraction of the bulk water signal (middle trace) reveals the contribution due to interfacial water (broad peak 45–130 meV) as well as the contribution due to biomolecules and other solutes (peaks at 11, 31, and 168 meV). The spike observed in this and other difference spectra at 67 meV is due to small errors in the energy transfer (time-of-flight) measurement between different runs. After removal of water by vacuum evaporation, the contributions to the IINS spectrum due to biomolecules and nonvolatile compounds can be observed (lower trace). (B) Double difference spectrum (lower thick line) after subtraction of the signal due to nonvolatile compounds from the interfacial water signal. The spectrum has been smoothed by binning across three data points. For comparison, the spectrum of ice Ih is also shown (upper trace).

bound to the lyophilized chymotrypsin, which may explain the weak signal in the 45–130 meV region; however, some protein vibrational bands may contribute weakly in this region, such as coupled protein skeletal and dihedral displacements.<sup>16,17</sup> Integrating for the different components in the librational band (45–130 meV) allowed us to estimate that the ratio of the bulk water/interfacial water signals in this sample was approximately 0.65:1

We investigated whether we could detect the IINS interfacial water signal in cells and tissues. Figure 2A shows data collected at TOSCA for yeast cells prepared as a paste. The total water

- (20) Michalarias, I.; Beta, I. A.; Ford, R. C.; Ruffle, S. V.; Li, J. C. *Appl. Phys. A* **2002**, *74*, 1242–1244.  
 (21) Michalarias, I.; Beta, I. A.; Li, J. C.; Ruffle, S. V.; Ford, R. C. *J. Mol. Liq.* **2002**, *101*, 19–26.  
 (22) Wu, G. L.; Beta, I. A.; Ma, J. B.; Li, J. C. *Appl. Phys. A* **2002**, *74* (Suppl.), S1267–S1269.

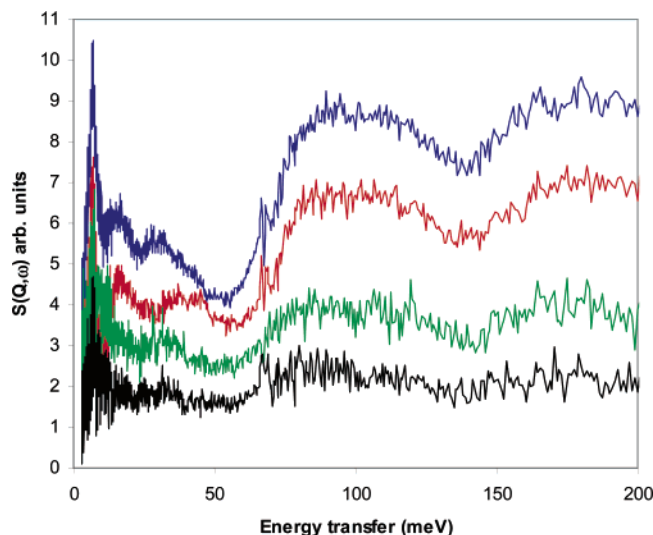


**Figure 3.** IINS spectra for other cells and tissues studied. The spectra show the interfacial water signal at 45–130 meV after subtraction of bulk water. The spectra represent (from top to bottom), cardiac muscle tissue, beetroot tuber tissue, *Chlamydomonas* cell pellet (in TAP medium), and spinach leaves. All the spectra have been normalized to the magnitude of the bulk water signal in the sample.

content of this yeast paste was about 67% by mass, as determined by vacuum-drying of the paste. The IINS spectrum for yeast cells is dominated by the bulk water signal; however, there was an interfacial water signal indicated by the broadening at the lower-energy edge of the librational band around 45–65 meV. After subtraction of the bulk water signal, the interfacial water signal in the librational region was revealed as well as the bands at  $\sim 30$  and  $\sim 170$  meV due to protein and DNA components of the cells (center trace in Figure 2A). A spectrum of a similar sample of yeast after removal of water by vacuum-drying is shown in the lower trace of Figure 1. Features of the spectrum due to nonvolatile cellular components can be discerned. The true interfacial water signal can be generated by a double difference spectrum, after subtracting the spectrum for the nonvolatile components as shown in Figure 2B. The interfacial water signal in yeast shares some of the features of the bulk water spectrum (ice Ih, upper trace in Figure 2B), but all the peaks are considerably broadened. Integration of the signals in the librational region was performed to estimate the relative signals due to interfacial and bulk water, and this indicated that 31% of the total water was interfacial. A duplicate experiment consisting of a separate yeast cell paste batch was also analyzed. In this case, an interfacial signal equivalent to about 24% of the total water was determined.

Other cell types and tissues were also investigated, and IINS data after subtraction of the bulk water signal is shown in Figure 3. The interfacial water signal is consistent in terms of its bandwidth and energy across the different tissue types surveyed, although its magnitude when normalized to the bulk water component varies considerably with tissue type. Cardiac muscle tissue had a large interfacial water signal, equivalent to 28% of the total water, similar to the yeast paste sample (Figure 2). In contrast, spinach leaves had an IINS spectrum that was almost entirely due to bulk water, although an interfacial water signal could still be identified (lowest trace, Figure 3). For these samples, the minor component due to biomolecules was not taken into account because of insufficient beamtime for record-

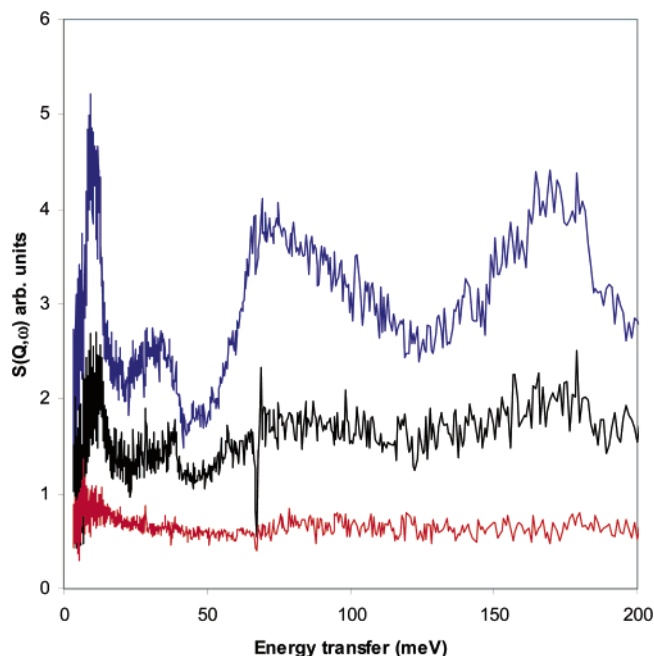


**Figure 4.** IINS spectra of solutes after subtraction of the bulk water component. Interfacial water signals arising in the 45–130 meV region are apparent. Upper trace, 2 M sucrose, middle trace 1 M sucrose, lower trace 1 M methanol. All spectra have been normalized using the bulk water signal magnitude.

ing spectra for lyophilized samples. However, it was found that this correction had only a marginal effect on the calculated ratio of interfacial/total water (e.g., for yeast paste [31% interfacial water] the value was 33% without the correction for nonwater components).

It is a reasonable hypothesis that small solutes such as ions and sugars could contribute to the interfacial water signal in the cells and tissues. Since cells contain an enormous range of such solutes, a complete survey using IINS would be impractical. We have carried out a limited survey thus far, and Figure 4 shows IINS spectra (after subtraction of the bulk water signal) for sucrose solutions and for a methanol solution. Sucrose is a common cellular solute and is present at significant levels in some plant tissues (see below). Methanol is rarely found in cells and tissues, but it was present at a 1 M concentration in the extracellular medium of one of the *Chlamydomonas* samples (see below). Sucrose at very high levels (2 M) yielded a large interfacial water signal, equivalent to about half the total water. The signal obtained with 1 M sucrose yielded a concomitantly smaller signal (see also Figure 5). The shape of this interfacial water signal is quite similar to that detected for biomolecules (Figure 1, ref 5) and cells and tissues (Figures 2 and 3). Sucrose is a disaccharide of molecular mass  $\sim 340$  Da, with many  $-\text{OH}$  groups that could potentially take part in extensive H-bonding to water, with approximately one interfacial water molecule per  $-\text{OH}$  group suggested from these data. By contrast, methanol with mass of 32 Da and a single  $-\text{OH}$  group will contribute much less at a 1 M concentration, and we can detect very little interfacial water signal in this sample (Figure 4, lower trace).

Figure 5 shows a summary of the IINS experiments with cells and tissues and solutes, including duplicate experiments where performed. In general, plant tissues had smaller interfacial water components, with fresh spinach leaves having only around 6% of total water as interfacial. Similarly, single celled plant material

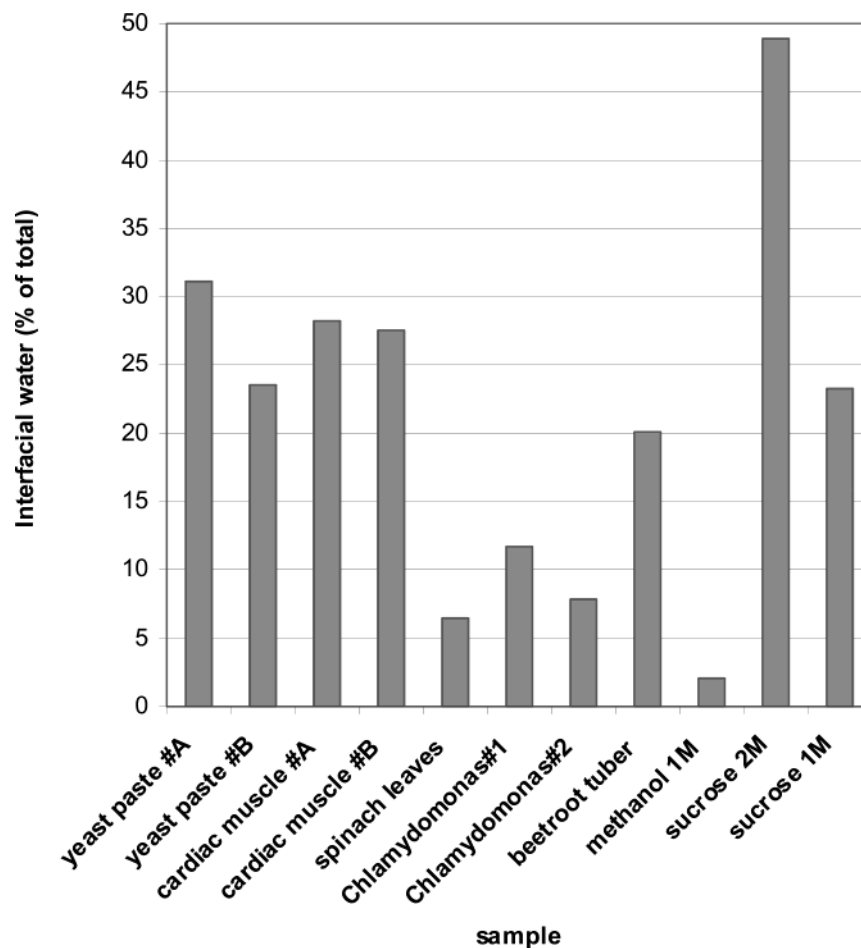


**Figure 5.** Summary of the relative interfacial water content in the different cells and tissues surveyed, and a comparison to standard solutions of small solutes. The interfacial water signal in the librational region of the IINS spectrum (45–130 meV) was integrated and then expressed as a percentage of the total water signal (interfacial plus bulk water) over the same region of the spectrum. The *Chlamydomonas* no. 1 and no. 2 samples were frozen under different conditions (see Methods section). For yeast and cardiac muscle, samples #A and #B represent duplicate experiments recorded during different visits to the instrumental station and represent different (fresh) material.

(*C. reinhardtii*) had low interfacial water content (8–12%). Beetroot tuber tissue had a higher interfacial water content (20% of total water). The data for plants are perhaps expected because plant cells are characterized by a large water-filled compartment, the vacuole, which is segregated from the rest of the cell contents.

The IINS spectra of the *Chlamydomonas* samples were recorded in two different media, one of which (TAP plus 3% methanol) allows freezing with subsequent recovery of cell viability ([www.biology.duke.edu/Chlamy/methods](http://www.biology.duke.edu/Chlamy/methods), R. T. Sayre, personal communication). We found that the cells could be frozen and thawed from the TAP-methanol medium with a recovery of about 28% viable cells. In contrast, freezing and thawing in TAP medium alone led to 0% viability. The interfacial water signal in TAP-methanol suspended cells (Figure 3, *Chlamydomonas* no. 2) was estimated to be slightly lower than in cells suspended in TAP alone (Figure 3, *Chlamydomonas* no. 1). The spectrum recorded for TAP medium alone was superimposable with the bulk water spectrum (Figure 1 trace A).

## Discussion

IINS spectroscopy has previously been applied to the study of hydrated biomolecules, but the major emphasis was on the biomolecules rather than the hydration water.<sup>16,17</sup> Hence, most

studies were performed in D<sub>2</sub>O to observe exclusively the (nonexchangeable) protons of the biomolecules. Recently, however, IINS measurements of H<sub>2</sub>O/DNA and H<sub>2</sub>O/proteolipid membrane mixtures have been carried out,<sup>5,6,20–22</sup> and a water component interacting with these biomolecules was identified and quantified. Recently, molecular dynamics simulations of interfacial water<sup>23</sup> have suggested that the characteristic broadening of the librational band may be due to a spread of hydrogen bond numbers and strengths between water and the solute atoms, with an increased rigidity in the structure surrounding the interfacial waters.

IINS data for water with a small globular protein has until now been unpublished. In Figure 1, we show that an interfacial water spectrum can also be observed for water/protein mixtures and that it is similar to the previously published spectra.<sup>5</sup> At a hydration level of 0.7 g water/g chymotrypsin, the interfacial water corresponds to 61% of the total water or about 0.43 g interfacial water/g protein. At similar hydrations levels of DNA, a similar ratio of bulk/interfacial water would be observed,<sup>5</sup> but in contrast, proteolipid membranes would show a larger bulk water signal and a smaller interfacial water signal. The explanation for the latter difference has been simplistically explained in terms of the overall geometry of the biomolecules/biomem-

(23) Pal, S.; Balasubramanian, S.; Bagchi, B. *Phys. Rev. E* **2003**, *67*, 061502.

branes. DNA can be modeled as a  $\sim 2$ -nm diameter cylinder, (and chymotrypsin as a 3.5-nm diameter sphere), whereas the proteolipid membranes resemble  $\sim 8$ -nm thick planar sheets that are several hundreds of nanometers wide. The latter structure therefore has a much lower surface area-to-volume ratio, and will bind interfacial water to a lower extent on a unit mass basis. Clearly other factors due to the surface properties of the macromolecules are also likely to influence the degree of interfacial water, but this geometrical approximation appears to be relatively robust. If we use a model for the interaction surface of chymotrypsin as a 35 Å diameter sphere with a surface area of  $\sim 3900 \text{ \AA}^2$ ,<sup>24</sup> then the interfacial water signal in trace C would correspond to about 1–2 layers (shells) of water molecules surrounding the protein. This corresponds to the extent of interfacial water determined for both DNA (1–2 layers) and proteolipid membrane samples (2–4 layers) when employing similar geometrical approximations.<sup>5</sup> However, the actual water-accessible area on the convoluted surface of chymotrypsin is considerably larger ( $\sim 11\,000 \text{ \AA}^2$ ) than that calculated for a sphere. If completely covered by water molecules, this surface area could theoretically account for almost all the water (bulk and interfacial) in the chymotrypsin sample. Since the bulk water corresponds to  $\sim 39\%$  of the total water as determined by IINS, this implies that water does not completely saturate the surface of the protein. Molecular dynamics simulations of water–protein interactions would assist the understanding of these data.

IINS spectroscopy of living cells and tissues is reported for the first time herein. Because of the long data collection times ( $>9$  h per sample), coupled with limited availability of experimental time at the station, a relatively limited selection of cells and tissues has thus far been tested. This has also limited duplicate experiments thus far to the cardiac muscle and yeast samples. The duplicate experiments were carried out  $\sim 12$  months apart on freshly prepared samples, and they give some indication of the biological variability in the experiments. There are problems for the quantitative interpretation of these data because of the complexity of the material:

(i) First, the technique cannot distinguish between intracellular and extracellular water, nor can it differentiate organellar compartments within the cell. For the single-celled samples (yeast and *Chlamydomonas*), it is inevitable that part of the bulk water signal will arise from the extracellular growth medium or cell wash buffer (e.g., TAP), a fraction of which is inevitably carried over after cell harvesting and sedimentation. For example, the carry over of the external water probably accounts for the variation observed in the estimates for interfacial water content in the yeast paste duplicates. Measurement of the morphology of the yeast paste sample was attempted by visualization by environmental scanning electron microscopy (ESEM). This revealed a close-packed array of deformed spheres. A close-packed array of hard spheres would have a volume external to the spheres of 26%, but the deformable nature of the yeast cells means that the actual external water volume is likely to be less than this. The interfacial water fraction determined by the IINS measurements is therefore likely to be a lower limit for the true value in the intracellular milieu for these samples.

For the tissues (cardiac muscle, spinach leaves, beetroot tuber), both intracellular and extracellular compartments of the tissue were sampled. The level of molecules (mainly soluble proteins and smaller solutes) in the extracellular milieu and vasculature in such material was difficult to gauge. Hence, for these samples we must presently work with a total tissue estimate for the interfacial and bulk water contents. Provided that the tissues are freshly prepared and are not dehydrated, then these estimates are likely to be less subject to variation than for yeast and *Chlamydomonas* samples.

Plants are known to have a low protein and high water content, and this is consistent with the IINS data showing a small water signal for these samples. Interestingly, the cytoplasm of plant cells is quite similar in its composition to the cytoplasm found in other organisms. The high water content of plant cells arises because they contain a large vacuole which in plants is a water-filled organelle occupying up to 80% of the total cell volume. The majority of the IINS water signal in these samples is likely to arise from the vacuole. The vacuole contains small solutes such as sucrose, ions, etc. This compartment has to maintain a marginally higher osmolarity ( $\sim 0.3$  OsM) than the surrounding cytoplasm to accumulate water and, hence, to regulate and maintain turgor pressure in the plant. A small interfacial water signal in the plant samples is therefore expected given the composition of the vacuolar compartment. The higher interfacial water content of the *Chlamydomonas* cells compared to the spinach leaves may be a reflection of their smaller vacuoles compared to that in vascular plants.<sup>25</sup> The interfacial water signal in the beetroot material is unexpectedly high and appears to indicate high levels of solutes strongly interacting with water in these tissues. Beetroot vacuoles are known to contain sucrose, but at levels  $\sim 0.2$  M that are too low to account for the large interfacial water signal. This appears to indicate that high levels of another solute may be present. A larger survey of plant storage roots by IINS could address this issue.

(ii) A second problem with quantitative analysis of the data for tissues and cells is that the measurements are necessarily recorded at cryogenic temperatures. It is possible that freezing could induce the redistribution of bulk and interfacial water (e.g., if ice Ih crystals grow at the expense of the interfacial water pool). For example, it has been proposed that slow, external ice crystal growth during freezing may extract water from cells, leading to dehydration.<sup>26</sup> Hence, for the majority of samples we studied, a rapid freezing ( $\sim 1$  s) by plunging into liquid nitrogen was carried out. For the *Chlamydomonas* samples, however, we used a very slow freezing rate and employed two different media for the cells, one of which (TAP-3% methanol) allowed some protection during the freezing of cells, with the retention of viability. We found that *Chlamydomonas* cells in cryoprotectant (TAP-methanol) medium had a slightly lower interfacial water signal than cells resuspended in TAP alone (the differences observed are probably within the errors due to media carryover as discussed above). There was no indication from these experiments that the cryoprotectant medium could influence the interfacial water signal nor that retention of cell viability during freezing was strongly linked to interfacial water levels.

(24) Mathews, B. W.; Sigler, P. B.; Henderson, R.; Blow, D. M. *Nature* **1967**, *214*, 652–656.

(25) Luykx, P.; Hoppenrath, M.; Robinson, D. G. *Protoplasma* **1997**, *198*, 73–84.

(26) Lovelock, J. E. *Biochim. Biophys. Acta* **1953**, *11*, 28–36.

Keeping the reservations listed above in mind, we compared the IINS data for cellular water with those obtained by other methods. Record and co-workers have estimated bulk and “bound” water components in *E. coli* cells using titrations that vary the external osmolarity and marker solutes that either can or cannot access the cytoplasm.<sup>27,28</sup> In this case, bound water is defined as the limiting amount of cytoplasmic water remaining at high osmolarity after a titration of nongrowing cells with increasing NaCl concentrations. This prokaryote has a protein concentration of  $\sim 200 \text{ mg mL}^{-1}$ , a total biomolecule concentration of  $\sim 200 \text{ mg mL}^{-1}$ , a bound water content of  $\sim 0.5 \text{ g/g}$  macromolecule, and a total cytoplasmic water content of  $\sim 2.3 \text{ g/g}$  macromolecule at the optimal osmolarity for cell growth (0.28 OsM). These data therefore show that bound water in the *E. coli* cell under normal conditions corresponds to about 22% of the total cell water, which is not inconsistent with the values for interfacial water observed for cardiac tissue (28%) and yeast (31–24%). Similarly, a bound water content of  $0.5 \text{ g/g}$  macromolecule in *E. coli*<sup>27,28</sup> corresponds closely with our measurements for interfacial water in yeast of  $0.62\text{--}0.48 \text{ g/g}$  macromolecule. Clearly, “bound” water as defined by Record et al. may not exactly correspond to “interfacial” water as determined by IINS herein. Nevertheless, quantitation of “bound” water in terms of g water/g biomolecules is useful as it will be less susceptible to variability in the preparation of samples, as discussed above.

(27) Record, M. T.; Courtenay, E. S.; Cayley, D. S.; Guttman, H. J. *Trends Biochem. Sci.* **1998**, *23*, 143–147.

(28) Cayley, D. S.; Guttman, H. J.; Record, M. T. *Biophys. J.* **2000**, *78*, 1748–1764.

In conclusion, we previously<sup>5</sup> predicted that the interfacial water content in cells and tissues could represent a significant fraction of the total water, and in some cases (e.g., in mitochondria) could approach 100% of the water. We have now tested this prediction experimentally using IINS. An estimate of  $\sim 25\text{--}30\%$  of water as interfacial was obtained from the data for yeast and cardiac cells. We expect this to be somewhat lower than the intracellular value because of interference from extracellular bulk water. The interfacial water is likely to be highly significant for cellular reactions and processes, but our data do indicate that tissues still contain a significant fraction of bulk water that is indistinguishable in terms of its vibrational properties from ice Ih. This is the case even in cardiac tissues where mitochondria are abundant. Further tissues and cells must be tested by IINS to get a better idea of the range of interfacial water content, and measurements of *E. coli* in particular are needed. A refinement of theoretical models of interfacial and bulk water in the cytoplasm is planned. The interfacial water spectrum is distinct from other known ice phases that have been studied by IINS,<sup>7,8</sup> but probably most closely resembles the IINS spectrum for high-density amorphous (HDA) ice.<sup>20,21</sup>

**Acknowledgment.** We thank Dr. S. Parker (ISIS, Rutherford Laboratory) for assistance at the TOSCA station and for useful discussions. This work was supported by the CCLRC (U.K.) via instrument time granted under the open access route.

JA0393269